Published in: *Water Research*, 2026, 289, Part A, 124885
https://doi.org/10.1016/j.watres.2025.124885

Sustainable Production of High-Purity Crystalline $FePO_4$ from Sludge for Battery Electrodes

Xuan Wang[a], Yijiao Chang[a], Zhu Liang[a], Anjie Li[b], Yiru Wu[c], Bohua Wen[c], Bing Li[a], Feiyun Sun[d], Xiao-yan Li[a,e*], Bruce E. Logan[f*], Lin Lin[a*]

[a] Institute of Environment and Ecology, Tsinghua Shenzhen International Graduate School, Tsinghua University, Shenzhen 518055, China.
[b] Key Laboratory of Water and Sediment Sciences of Ministry of Education, State Key Laboratory of Water Environment Simulation, School of Environment, Beijing Normal University, Beijing 100875, China.
[c] Institute of Materials Research, Tsinghua Shenzhen International Graduate School, Tsinghua University, Shenzhen, 518055, China.
[d] State Key Laboratory of Urban Water Resource and Environment, Harbin Institute of Technology (Shenzhen), Shenzhen, 518055, China.
[e] Environmental Engineering Research Centre, Department of Civil Engineering, The University of Hong Kong, Pokfulam, Hong Kong, China.
[f] Department of Civil and Environmental Engineering, The Pennsylvania State University, University Park, Pennsylvania, 16801, United States.

* Corresponding authors:
Xiao-yan Li, lixiaoyan@sz.tsinghua.edu.cn
Bruce E. Logan, blogan@psu.edu
Lin Lin, linlin00@sz.tsinghua.edu.cn

Abstract: A growing demand for phosphorus to produce lithium iron phosphate ($LiFePO_4$) battery electrodes has raised concerns about further depletion of limited resources of mined phosphorous. Primary sludge from wastewater treatment plants could provide a highly sustainable source of P for battery electrodes but this material has not been successfully used for P recovery to make $LiFePO_4$ electrodes. The major obstacles for recovering P from typical waste sludges have been the difficulty and low efficiency in P extraction, and obtaining $FePO_4$ of sufficient quality (purity) and durability for use in battery electrodes and avoiding contamination by other metals. To demonstrate the feasibility using sludge to produce high quality $LiFePO_4$, we developed a new approach based on upfront P capture using Fe-enhanced primary sedimentation, followed by P extraction from the P-rich primary sludge using acidogenic fermentation, and then selective precipitation of P and Fe using acidic and highly oxidative conditions (pH=2, with H_2O_2 addition). Chemical analysis of the precipitate showed negligible metal impurities. The solids were sintered to produce crystalline $FePO_4$ with a purity of 99.3%, which surpassed that of typical industrial sources (93.8%). The performance and durability of the recovered $FePO_4$ was assessed for making $LiFePO_4$/C cathodes. The battery performance based on energy discharge capacity after 50 cycles of 143 ± 1 mAh/g was not significantly different (p = 0.14) than that of the control prepared with standard industrial $FePO_4$ (140 ± 2 mAh/g). An economic assessment showed that production of $FePO_4$ for batteries had good economic advantages compared to P recovery for use in fertilizers. These findings demonstrate for the first time that battery-grade $FePO_4$ can be economically produced from the phosphorus captured in Fe-enhanced primary sludge, and that the performance of electrodes made using this wastewater-derived material was comparable to that using conventional materials.

Keywords: Wastewater sludge; $FePO_4$; $LiFePO_4$ cathode; Selective Fe-P precipitation; Phosphorus recovery

1. Introduction

Driven by the increasing demand for power batteries and energy storage capacity, the production of lithium-ion batteries (LIBs), particularly those using $LiFePO_4$ (LFP) as the cathode material is rapidly increasing. For example, the annual production of $LiFePO_4$ in China has increased by more than 17 times in the past five years, consuming 2,371,900 tons of $FePO_4$ in 2024 (CNMIA, 2025). The LFP cathode material, $FePO_4$, possesses a high market price of ~$3200/t (http://img.baiinfo.com), and demand for this material is forecast to grow in coming years. The production of LFP is currently dependent on mined phosphorus (P), which is being used at a rate that could deplete known sources by the end of the century (Chowdhury et al., 2017; Zhou et al., 2025). Exploring cost-effective substitutes from recycled sources for P ore-based $FePO_4$ is therefore essential to resolving the conflict between the growing LIB industry and P resource conservation (Li et al., 2018).

Phosphorus can be locally recovered from sewage treatment plants as a sustainable alternative to mined sources often at distant locations. Sludge collected from the treatment processes contains enriched concentrations of P due to its removal from wastewater (Uysal et al., 2010). Efforts to recover P from wastewater sludge have primarily been focused on producing P-based fertilizers such as struvite and vivianite (Van Loosdrecht and Brdjanovic, 2014; Taddeo et al., 2018; Li et al., 2021). However, there are several drawbacks for economical P recovery for fertilizers, including the low efficiency of P extraction (10%–50%) (Wu et al., 2019), high costs of chemical reagents (HCl/H_2SO_4, NaOH, and $MgCl_2$), and potential risks of heavy metal contaminants and per- and polyfluoroalkyl substances (PFAS) in the products (Taddeo et al., 2018). The low market value of these fertilizers (US$200–300/t) (https://www.chinabgao.com/) make it difficult to make P recovery profitable, and the market for the product is challenged by an inconsistent demand. In contrast, battery-grade $FePO_4$ has a market price 10 times higher than P-fertilizers, and thus it could be a much more economically advantageous product. It is estimated that the recovery of P from wastewater sources could potentially supply the domestic LFP industry with up to 1.45 times its current P usage in China (Meng et al., 2018; Fan et al., 2020; Ouikhalfan et al., 2022).

Chemical methods have previously been used for P extraction from waste sludge for $FePO_4$ production (Hu et al., 2023; Zheng et al., 2023; Zou et al., 2024). However, these approaches have produced products that have poor purity or low performance in LFP batteries. For example, P recovered from sludge incineration produced solids containing 92.9% $FePO_4$ (Hu et al., 2023), but the resultant battery performance reached only 106 mAh/g in terms of the maximum discharge capacity, well below the minimum discharge requirement of 136 mAh/g for energy storage applications (Pokhrel et al., 2018; Zou et al., 2024). The need for large amounts of chemical reagents such as H_2SO_4 acid to dissolve P from waste sludge and the additional requirement for iron currently makes the process costs uneconomical (Zheng et al., 2023; Zou et al., 2024).

Changing operational procedures at many wastewater treatment plants operations to make their operation more sustainable through reduced carbon emissions and nutrient losses offers a new opportunity to more easily capture and use both phosphorus and iron. In these two-stage systems the first stage captures increased amounts of carbon and

nutrients in the primary sludge, resulting in the second stage having enhanced effluent quality at reduced energy consumption (Wang et al., 2015; Dunn, 2024; Zheng et al., 2024). Technologies employed in the first stage for energy-saving and resource recovery include high rate activated sludge (HRAS) (Lee et al., 2025), chemically enhanced primary sedimentation (CEPS) (Taboada-Santos et al., 2020), and chemical phosphorus removal (CPR) (Wang et al., 2021). The first stage of treatment, when using iron-based coagulants, produces sludges containing iron hydroxy phosphates (Zhang et al., 2019; Li et al., 2020). The weakly bound P in the P-capturing primary sludge produced in the first stage process is more amenable for P release back into the liquid phase for recovery, than strongly bound P in waste sludge and incineration ashes used in previous chemical extraction tests (Li et al., 2018a; Taboada-Santos et al., 2020; Zou et al., 2024). Iron coagulated sludge is already rich in iron, in addition to phosphorus, making it potentially more suitable and economical for recovery and production of high-purity $FePO_4$ for LFP batteries than bio-sludge-based waste sludge and other sources.

In this study, we examined extraction and purification of $FePO_4$ using solids obtained from an iron coagulated sludge produced by a two-stage treatment process. To release the P and Fe from the upfront P-capturing primary sludge we used acidogenic fermentation step (Lin et al., 2017a; Li et al., 2018b; Xue et al., 2025) to avoid the need for strong acids for leaching used in previous chemical approaches. This fermentation step was followed by selective Fe-P re-precipitation at acidic pH 2 that differed from previous processes by using a strong oxidizer (H_2O_2) to enhance selective $FePO_4$ precipitation with little impurities. We then sintered the precipitates to produce $FePO_4$ and conducted analyses to verify the lack of metal contaminants. The electrochemical performance of $LiFePO_4$/C cathodes made using the recovered $FePO_4$ as the precursor was examined and compared to a control using a commercial reagent $FePO_4$. The overall recovery $FePO_4$ process was also evaluated for its environmental and economic benefits considering mining costs and transportation.

2. Material and methods

2.1 Chemicals and materials

The primary sludge was collected from a pilot-scale resource recovery plant at Siu Ho Wan Sewage Treatment Works (SHWSTW), Hong Kong. The SHWSTW employs chemically enhanced primary sedimentation by dosing $FeCl_3$ at around 10 mg-Fe/L as the chemical coagulant for treating domestic wastewater. Similarly, in the pilot plant with a capacity of 10 m^3/d, $FeCl_3$ was added for the first-stage primary treatment, with a higher dosage of 15 mg-Fe/L applied to achieve greater levels of organic carbon capture and P removal from the wastewater, without pH adjustment. The continuous treatment process involved a rapid mixing step for 2 min, followed by slow mixing for 15 min, and then settling for 1 h (Lin et al., 2017a; 2017b). The sediment was collected from the sedimentation tank as the Fe-enhanced primary sedimentation sludge, or Fe-enhanced primary sludge (FEPS), achieving more than 90% P removal from the wastewater. For comparison, waste bio-sludge (WBS) was also collected as a P-containing waste from the secondary sedimentation tank of Nanshan Wastewater

Treatment Plant in Shenzhen, China. The basic properties of the obtained sludge samples are provided in Table S1. For the subsequent experimental work, the following chemical reagents were purchased from Sigma-Aldrich (Shanghai, China): ferric chloride ($FeCl_3$, 99%), iron phosphate ($FePO_4$, 99%), lithium carbonate (Li_2CO_3, 99.99%), glucose ($C_2H_{12}O_6$, 99%), sulfuric acid (H_2SO_4, GR), nitric acid (HNO_3, GR), hydrogen peroxide (H_2O_2, 30%), ethanol (C_2H_6O, AR), carbon black (99%), polyvinylidene fluoride (99%), and N-methyl pyrrolidone (AR).

2.2 P and Fe release from the sludge by acidogenic fermentation

The sludge obtained from the wastewater treatment plant was processed by acidogenic fermentation under naturally occurring anaerobic conditions for biological extraction of P (mainly PO_4^{3-} and HPO_4^{2-}), together with Fe (mainly Fe^{2+}) (Li et al., 2018b; 2019). Rice-rich food waste, a type of highly biodegradable carbohydrate-rich food waste (FW), was added for co-fermentation with the sludge. This FW-based approach has been reported as a cost-effective method to enhance acidogenesis and promote chemical release from the sludge (Li et al., 2020; Rathuka et al., 2024; Naveen et al., 2024). The rice-rich FW was collected from a student canteen of the University Town in Shenzhen, China, and its main properties are provided in Table S1. FW was added at various FW:sludge ratios to increase the initial organic matter concentration (measured as total volatile solids, VS) of the mixture for fermentation, resulting in initial organic matter concentrations of 6 and 12 g VS/L. For fermentation each 550-mL serum bottles were each filled with 450 mL of the mixed suspension and 50 mL of seed from a laboratory acidogenic fermenter. The fermentation bottles were capped with rubber stoppers and placed in a temperature-controlled shaker operating at 37 °C and 180 rpm. During the anaerobic fermentation process, the sludge mixture underwent hydrolysis and acidogenesis, producing volatile fatty acids (VFAs) to lower the pH, and dissolving Fe and P into the solution. The fermentation experiments were carried out for 6 d and samples were collected every 12 h to monitor the fermentation performance, specifically the release of Fe and P into the liquid phase of the mixture. In addition to FEPS, co-fermentation experiments were also conducted on WBS under the same FW loading conditions.

2.3 Recovery of Fe and P and preparation of crystalline $FePO_4$

After fermentation, the sludge-FW mixture was centrifuged at 3,700×g for 5 min, and then the supernatant was filtered (0.45-μm pore diameter membrane, Millipore Sigma). P and Fe in the filtrate were then recovered via selective Fe-P re-precipitation under strong acidic and oxidative conditions. To drive Fe-P precipitation with minimal chemical impurities, we used a new procedure developed to recover Fe-P from spent LFP battery electrodes and not previously used for chemical recovery from sludges (Chen et al., 2017; Yin et al., 2025). The pH of the filtrate was first adjusted from 4.5 to 2.0 with sulfuric acid (9 M H_2SO_4, added dropwise). We then added 1% H_2O_2 (30%) to oxidize Fe(II) to Fe(III) at 40 °C, resulting in the formation of yellowish precipitates (Zhang et al., 2022). Under these strong oxidative conditions at low pH, P primarily precipitates with Fe(III), with minimal co-precipitation with other metal ions (Lou et al.,

2021; Bahgat et al., 2024). After stirring intensely for 2 h, the suspension was left undisturbed for 12 h. The precipitates were obtained by filtration, with the collected solids washed three times with ultrapure water before drying at 105 °C for 24 h (Mao et al., 2015; Zhu et al., 2014). The Fe-P precipitate was sintered at 700 °C for 12 h in air in an oven enabling further purification through oxidation of organics (Chen et al., 2022), producing the final crystalline $FePO_4$ product. For comparison with the above selective Fe-P re-precipitation procedure, P and Fe were also recovered from the filtrate through conventional precipitation by raising the solution pH to 7.0 using aqueous ammonia (Lin et al., 2017b). The resulting precipitate was then collected and subjected to the same sintering treatment.

2.4 Synthesis of the $LiFePO_4$/C cathode materials

$LiFePO_4$/C was synthesized using three raw materials: $FePO_4$, Li_2CO_3 as the Li source, and glucose as the C source (Tu et al., 2025). The molar Fe:P:Li ratio was 1:1:1.04, with glucose accounting for 20 wt% of the total mass (Zhou et al., 2017). The suitability of the recovered $FePO_4$ for use in battery electrodes was examined and compared to commercially available $FePO_4$. The three raw materials ($FePO_4$, Li_2CO_3, and glucose) were mixed by ball milling at 400 rpm for 8 h with ethanol as a dispersant and then dried at 80 °C for 12 h in an oven. Afterward, the mixture was preheated at 400 °C for 4 h and sintered at 700 °C for 12 h in an Ar/H_2 (5%) atmosphere to produce the $LiFePO_4$/C cathode materials (Veeken and Hamelers, 1999; Wang and Sun, 2012), according to the following equation:

$$FePO_4+Li_2CO_3+C_6H_{12}O_6 \xrightarrow{Ar/H_2} LiFePO_4/C+H_2O+CO\uparrow+CO_2\uparrow \quad (1)$$

2.5 Chemical analysis

The pH of the solution was measured using a pH meter (Starter 310, Ohaus, USA). The total solids (TS), volatile solids (VS), soluble chemical oxygen demand (SCOD), total phosphorus (TP) and orthophosphate P (PO_4^{3-}-P) were determined in accordance with Standard Methods (APHA, 2005). The total organic carbon (TOC) concentration was measured by a TOC analyzer (Elementar Vario TOC Select, Germany). VFAs produced during the fermentation process were quantified using a gas chromatograph (GC-2014, Shimadzu, Japan) following the details of Lin et al. (2017a). The concentrations of Fe^{2+} and total Fe in the suspensions were analyzed using the phenanthroline method (Lovley and Phillips, 1988). The contents of chemical elements (i.e., Fe, Al, Ca, Na, K, P, Si Mg Mn, Cu, and S) in the solid phases of the Fe-P precipitates, crystalline $FePO_4$ particles, and synthesized $LiFePO_4$ samples were determined with the inductively coupled plasma-optical emission spectrometry (ICP-OES, 720ES, Agilent, USA). Prior to analysis, the samples were digested using HNO_3 and H_2O_2 (30%). The experimental data are reported as the averages and standard deviations of the results obtained in triplicate tests.

2.6 Materials characterization

The mineral phases and structures of the synthesized materials were characterized with X-ray diffraction (XRD, Rigaku Ultima IV, Japan). The micro-morphology of the

materials was characterized through scanning electron microscopy (SEM, SU8010, Hitachi, Japan) and transmission electron microscopy (TEM, JEOL F200, Japan). X-ray photoelectron spectroscopy (XPS, Thermo Scientific Nexsa, USA) was applied to determine the atomic valences of the recovered $FePO_4$ product. The thermogravimetric behavior was analyzed using differential scanning calorimetry (DSC, Mettler 1100LF, Switzerland) on the organic content in the Fe-P precipitates. The Visual MINTEQ 3.1 model was used to calculate the concentrations of PO_4^{3-}-P in the solution in a pH range of 0.0–12.0.

2.7 Electrochemical measurements

The synthesized $LiFePO_4$/C cathode was used to assemble button batteries for electrochemical performance testing. The active substance ($LiFePO_4$/C or $LiFePO_4$), polyvinylidene difluoride, and acetylene black, at a weight ratio of 8:1:1, were ground homogeneously in an agate mortar, and the ground mixture was then mixed with the N-methyl-2-pyrrolidinone liquid to form a slurry (Chang et al., 2024; Song et al., 2025a; 2025b). The slurry was then placed onto aluminum foil at a uniform thickness of 0.02 mm using an automatic film coating machine (MRX-TM300, Shenzhen Mingruixiang Automation Equipment, China) and then dried in an oven at 80 °C for 12 h. The aluminum foil with the coating layer was cut into uniform discs 12 mm in diameter to obtain the cathode for the electrochemical test. In an Ar-filled glove box, coin-type 2025 half-cells were assembled with the as-prepared cathode and lithium foil as the anode. The cathode and anode of the battery were spaced out by a separator (Celgard 2500, 19 mm in diameter), and 1 mol/L $LiPF_6$ in a mixture of ethylene carbonate, dimethyl carbonate, and ethyl methyl carbonate (at a volume ratio of 1:1:1) was prepared as the electrolyte. The charge and discharge performances of the battery cells were evaluated between 2.0 and 4.3 V using a LAND battery test system (CT3002A, Wuhan LAND Electronic, China). All electrochemical tests were carried in triplets, for which the active material has a loading mass of 8-10 mg/cm^2.

3. Results and discussion

3.1 Extraction and production of Fe-P precipitates

3.1.1 Acidogenic fermentation for Fe and P dissolution

The sludge obtained from the wastewater treatment coagulated using iron salts was combined with FW and an acidogenic fermentation was used to facilitate the dissolution of P and Fe species into solution. Fermentation under anaerobic conditions produced primarily VFAs (Lin et al., 2017b) and resulted in an acidic solution at a pH ranging 4.4-6.4, depending on the total organic concentration (6 and 12 g VS/L) (Fig. S1). Specifically, the pH values after fermentation for the mixtures were 6.4 for FEPS, 4.4 for FEPS with FW addition, 6.9 for WBS, and 4.4 for WBS with FW addition. Under these conditions, insoluble Fe(III) was converted to soluble Fe(II) by dissimilatory iron reducing bacterial, and P released primarily as orthophosphate (PO_4^{3-} and HPO_4^{2-}) ions (Li et al., 2019). Over time Fe^{2+} and PO_4^{3-} continuously dissolved into the supernatant (Fig. 1a and 1b), with the largest concentrations obtained with the highest initial organic

loading concentration of 12 g VS/L, releasing 265±2 mg-Fe/L and 149±2 mg-P/L into the supernatant. The proportion of Fe and P dissolved into the supernatant increased with the initial organic concentration for co-fermentation, reaching 80% of Fe and 82% of P from the P-rich FEPS for the loading case of 12 g VS/L (Fig. 1c). In contrast, the WBS discharged from biological treatment without iron addition resulted in significantly lower P release efficiency under the same organic loading conditions, with only 14% of P dissolved from the sludge, similar to previous reports (Xue at al., 2025). During the fermentation process, the molar ratio of Fe:P in the supernatant of sludge generally increased over time, indicating a slower release of Fe than P (Fig. 1d). For FEPS, the Fe:P ratio in the supernatant was very close to unity (0.98) at the highest loading after 132 h of fermentation. While chemical leaching from the sludge using concentrated H_2SO_4 can achieve similar Fe and P dissolution efficiencies (~80%) (Fig. S2), the use of chemical reagents is avoided here with the acidogenic fermentation.

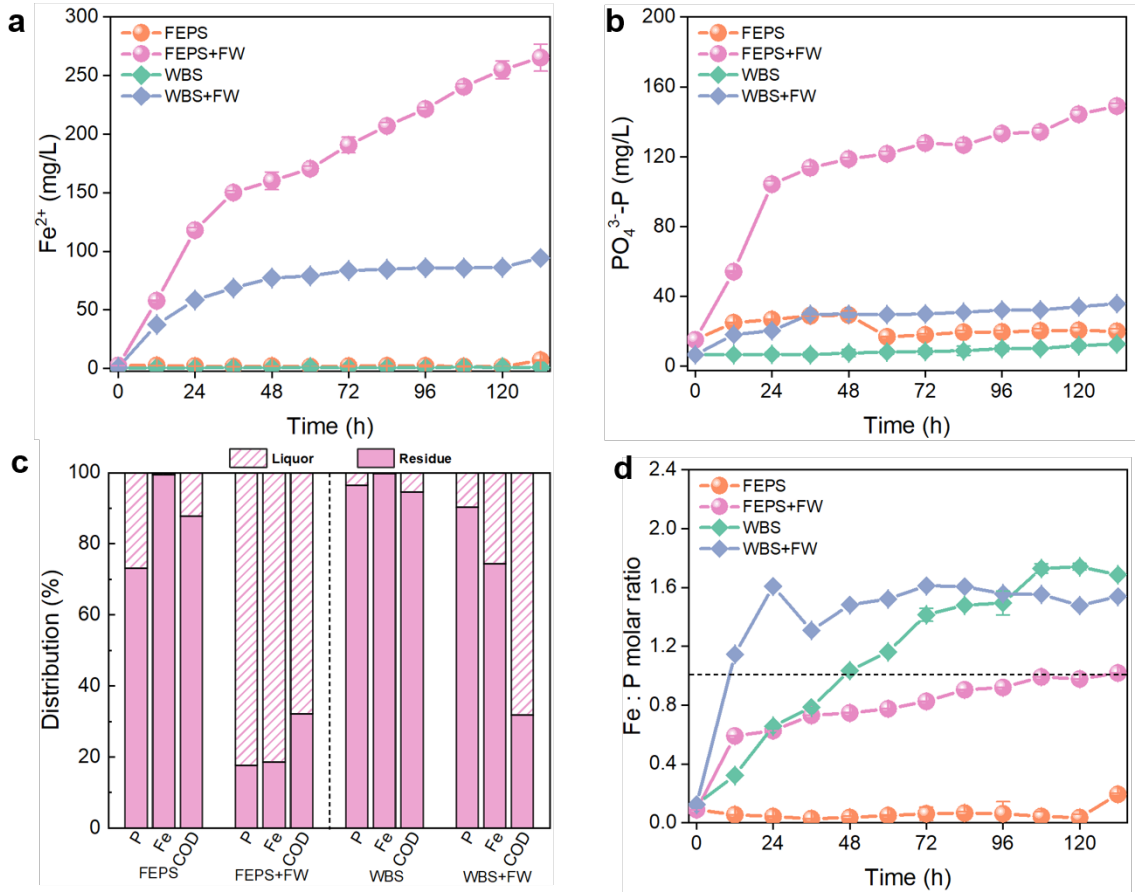


Fig. 1. Acidogenic co-fermentation of the sludge mixture based on the initial organics concentration based on volatile solids (VS): (a) Fe^{2+} and (b) PO_4^{3-}-P in the fermentation supernatant; (c) P, Fe, and COD distributions in the supernatant and sludge residue at the end of fermentation and (d) the Fe^{2+}:PO_4^{3-}-P molar ratio in the fermentation supernatant.

3.1.2 Selective precipitation of Fe and P from the supernatant

The fermentation supernatant was adjusted to pH 2 using a small amount of acid (i.e., 1.8 mmol/L, around 5-10% of that typically used in acid extraction processes), followed by H_2O_2 addition to produce strong oxidizing conditions for selective Fe-P re-

precipitation, where H_2O_2 serves to oxidize Fe^{2+} to Fe^{3+}, promoting efficient Fe-P precipitation. The dosage, reaction time, and temperature were optimized to ensure complete Fe^{2+} oxidation while minimizing phosphate loss and undesirable oxidation of organic matter. Up to 79% of the Fe (209±2 mg/L) and 81% of the P (121±1 mg/L) were precipitated and recovered for the VS = 12 g/L sample (Fig. 2a), achieving an overall P recovery ratio as high as 66% from FEPS. The concentrations of other metal ions in the supernatant, including Ca, Na, and Mg, only slightly decreased in the solution (<34±5 mg/L in total) after Fe-P precipitation (Fig. S3), indicating their limited precipitation with Fe and P under these conditions. The co-precipitation method enables the precipitates to achieve uniform nanoscale sizes. SEM images of the yellowish precipitates showed slightly spherical particles with diameters of 100–150 nm (Fig. 2b). In addition, these nanosized particles tended to agglomerate into larger clusters, consistent with the observations reported by Bahgat et al. (2024). The XRD pattern did not show characteristic peaks for crystalline structures (Fig. 2d), indicating amorphous phases of the Fe-P precipitate. An ICP-OES analysis confirmed that P and Fe were the predominant inorganic elements present in the precipitate, at a molar ratio of 1:0.96, followed by S (6.0%), Na (1.9%), Ca (1.2%), K (0.9%), and Al (0.6%) based on their atomic ratios relative to P (Fig. 2e). These percentages of impurities in the precipitate were considerably lower than those in the collected sludge (Fig. S4). This level of impurities was much lower than that of the other recovered P-products reported in literature, such as vivianite (Ca 4.8% and Mg 6.4% relative to Fe) (Li et al., 2021) and struvite (Zn 0.6% and Hg 0.7% relative to Mg) (Uysal et al., 2010).

The low amounts of these chemical impurities obtained here in the precipitated solids were due to the acidic pH and strong oxidation conditions by using H_2O_2. Under these conditions the majority of P tends precipitates as $FeHPO_4^+$ and $FeH_2PO_4^{2+}$ (Fig. 2f). Precipitating Fe and P from water is generally regarded as straightforward, typically forming vivianite ($Fe_3(PO_4)_2$) (Lin et al., 2017b; Li et al., 2018a). For comparison, additional tests were conducted using simple precipitation by adjusting the solution pH to 7, a common method for recovering P-fertilizers from sludge suspensions (Liao et al., 2024). When the pH was increased from 4.4 to 7, the solids, identified as vivianite (Lin et al., 2017b), exhibited particle sizes ranging 3-7 μm, which were much larger than particles formed with acid treatment under H_2O_2 addition (Fig. 2c). P and Fe remained the dominant inorganic elements in the precipitate, present at a molar ratio of 1:2.7 (Fig. 2e). However, as expected, co-precipitation readily occurred between P and the numerous impurity ions in the solution, including Ca (31.4%), Mg (4.6%), Mn (2.6%), S (2.1%), Si (1.9%), Na (0.8%), Al (0.7%), and K (0.2%). These high levels of impurities co-precipitated at pH 7 would significantly compromise the quality of $FePO_4$ to be recovered. Therefore, by setting a low pH of 2.0 for Fe-P precipitation can effectively minimize the co-precipitation of competing metal ions. However, as observed here (Figs. 2a and S3), precipitation would not occur under such strongly acidic conditions at pH 2. In this content, oxidizing Fe(II) to Fe(III) with H_2O_2 enabled P to precipitate with Fe even under acidic conditions at pH 2, with minimal co-precipitation with other impurity ions (Fig. 2e).

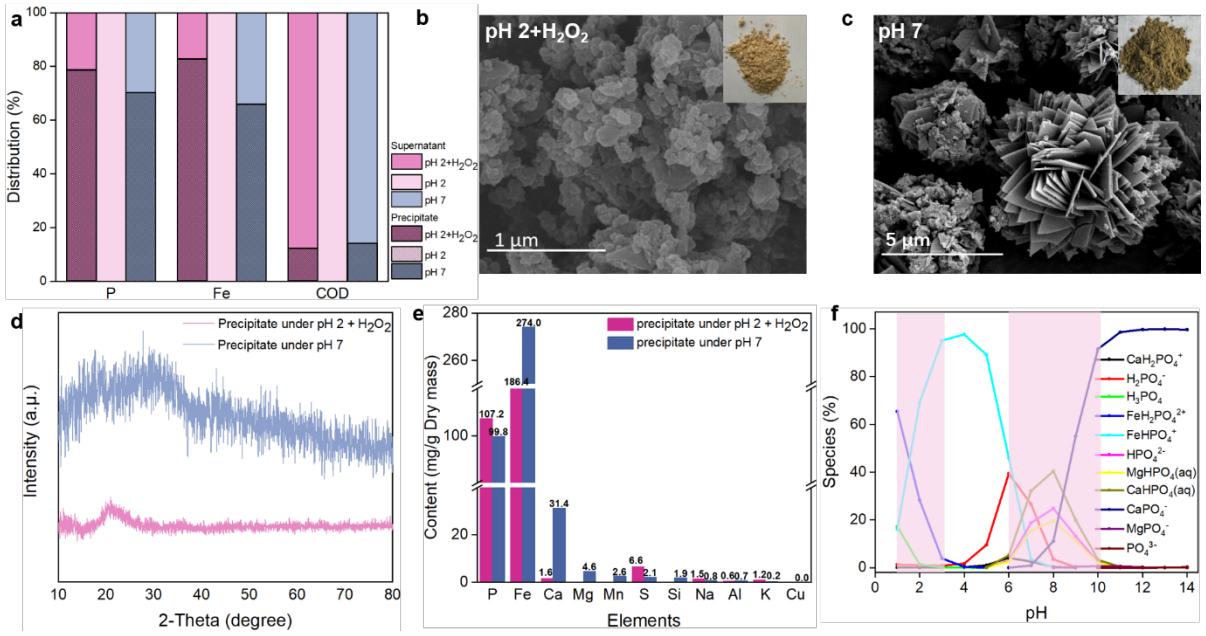


Fig. 2. Recovery of the Fe-P precipitate from the fermentation supernatant liquor: (a) distributions of P and Fe concentrations and organic contents in the supernatant and Fe-P precipitate after selective Fe-P re-precipitation under pH 2 with H_2O_2 addition, pH 2, and pH 7 conditions, (b) and (c) SEM images of the recovered Fe-P precipitate at pH 2 with H_2O_2 addition and pH 7 (inset: photograph of the precipitate powder), (d) XRD pattern and (e) ICP-OES analysis of the element content of Fe-P precipitate formed at pH 2 with H_2O_2 addition and pH 7, and (f) prediction of various complexation chemical species in the presence of phosphate ions as a function of pH.

3.2 Sintering of Fe-P precipitate for $FePO_4$ formation and purification

The Fe-P precipitates were sintered at 700 °C to remove organic matter (initially 48% by mass) and to crystalize the $FePO_4$ (Wang and Sun, 2012; Zhou et al., 2017). XRD patterns obtained following sintering indicated successful transformation of the precipitate from an amorphous to a crystalline $FePO_4$ structure (Fig. 3a). The sharp and intense peaks observed at 20.38°, 25.93°, 38.14°, and 48.58° corresponded with the characteristic peaks for crystalline $FePO_4$ (PDF # 77-0094), and no other peaks were detected. The morphology of the crystals observed using SEM indicated large spherical particles 200–250 nm (Fig. 3b), suggesting $FePO_4$ crystallization and growth with the elevated temperature (Laouini et al., 2025). Based on analysis using differential scanning calorimetry (DSC) (Fig. 3c) at temperatures greater than 530 °C up to 44% of the total mass was lost due to evaporation of crystal water (Zhu et al., 2014) and oxidation of organic matter. The decrease in total organic carbon (TOC) from 208 mg/g to 0 in the sintered product indicated the complete elimination of organics. Based on the mass losses, the organic matter accounted for 20.8% of the total mass of the precipitate, while crystal water accounted for 21.0%, closely matching the theoretical crystal water content of 20% for strengite ($FePO_4 \cdot 2H_2O$). Two endothermic effects were observed from the DSC curves at 190 °C and 280 °C, which correlated with the losses of water and sulfur, respectively. Two additional endothermic effects were observed in the DSC curves at

360 °C and 500 °C that correspond to the differential thermogravimetric peaks, with these two peaks attributed to the oxidation of carbonaceous organics. Both the DSC and thermogravimetric curves remained stable after 530 °C for the phase transition of the $FePO_4$ precipitate from its amorphous phase to the crystalline phase (Yuan et al., 2024; Boonchom and Puttawong, 2010).

XRD analysis of the particles produced by sintering using the Fe-P precipitate produced by pH adjustment to pH 7 without H_2O_2 treatment indicted the transformation of amorphous precipitate into crystalline Fe-P compounds ($Fe_4(P_4O_{12})_3$) (Fig. S5), but also indicated peaks of impurities such as $Ca_9Fe(PO_4)_7$. ICP analysis and SEM mapping further confirmed high contents of impurities in the sintered product (Fig. S5). Therefore, the $FePO_4$ crystal obtained from the Fe-P precipitate formed at pH 2 with H_2O_2 addition was used as the precursor for the synthesis of LFP cathodes.

After sintering of the Fe-P precipitate, the mass content of Fe increased from 186 mg/g to 359 mg/g in the $FePO_4$ product, and P increased from 107 to 207 mg/g (Fig. 3d). EDS elemental mapping (Fig. S6) indicated a relatively uniform distribution of Fe, P, and O in the $FePO_4$ product. XPS (Figs. 3f, and S7) further confirmed the presence of Fe, O, and P elements. The characteristic peaks in the XPS spectra were assigned to Fe $2p_{1/2}$ and Fe $2p_{3/2}$ with binding energies of 726.63 and 713.13 eV, respectively, indicating a +3 valence of Fe (Zeng et al., 2017). The content of $FePO_4$ in the sintered product was 99.3% (Fig. 3d), which was higher than the standard of industrial battery-grade $FePO_4$ in China (HG/T 4701-2021) (≥93.8% at an Fe:P ratio of 0.96–1.0). These results show that air sintering at 700 °C was an effective method for producing crystalline $FePO_4$ suitable for battery applications.

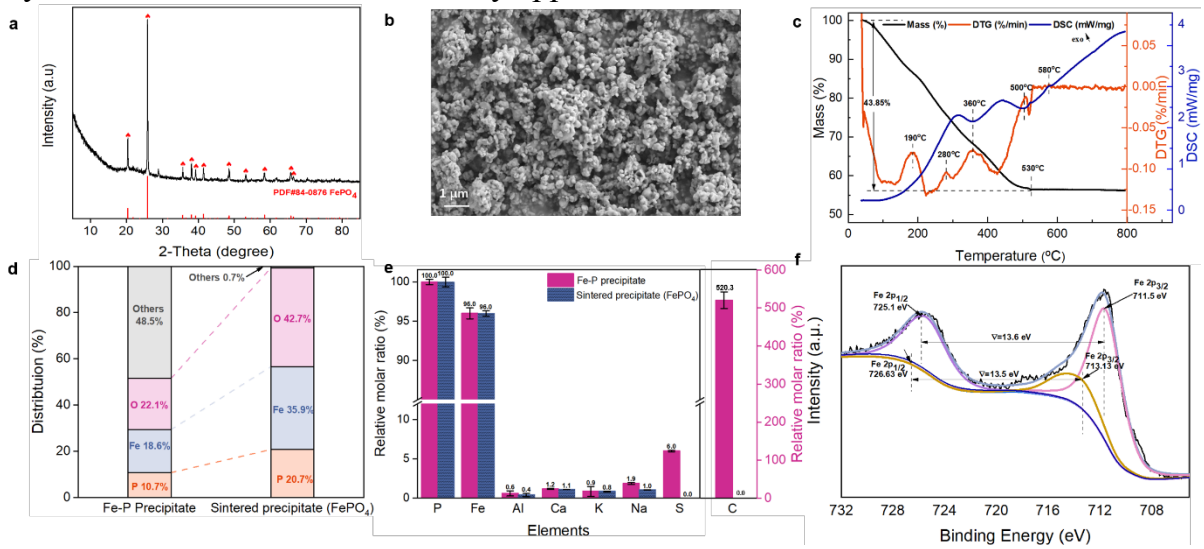


Fig. 3. Characterization of the sintered precipitate - crystalline $FePO_4$ product: (a) XRD profile, (b) SEM image, (c) thermogravimetric behavior and DSC analysis of the sintered product ($FePO_4$), (d) elemental distributions of P, Fe, O, other metals, and impurities in the sintered $FePO_4$ product, (e) relative molar ratios of elements (relative to P) in the recovered Fe-P precipitate and $FePO_4$ product, and (f) high-resolution XPS spectrum of the Fe 2p regions of the $FePO_4$ product.

3.3 Use of the $FePO_4$ product for $LiFePO_4$/C cathodes

3.3.1 Characterization of the $LiFePO_4$/C cathode material

Cathodes made with $LiFePO_4$/C using the recovered $FePO_4$ were examined based on morphology and chemical content compared to those of a commercially available material. The $LiFePO_4$/C particles prepared using the recovered $FePO_4$ displayed a similar near-circular lamellar structure (Fig. 4a and 4b). These particles of 200-250 nm (Fig. 4a) were smaller than those (500-900 nm) prepared using the commercial reagent $FePO_4$ (Fig. 4b). Smaller particles are more favorable for ion transport through $LiFePO_4$ cathodes (Phan et al., 2019; Akhmetova et al., 2024). The TEM images of the two $LiFePO_4$/C samples in Fig. 4c and 4d indicate a carbon coating with a thickness of 8-14 nm, which can improve conductivity of the cathode material and help to suppress the overgrowth of $LiFePO_4$ particles (Wang and Sun, 2012). The particles prepared from both the recovered $FePO_4$ and reagent $FePO_4$ exhibited almost identical XRD patterns without impurity peaks (Fig. 4e). The wide scan XPS spectra confirmed the similar presence of Li, Fe, O, and P elements in both of these samples (Fig. 4f).

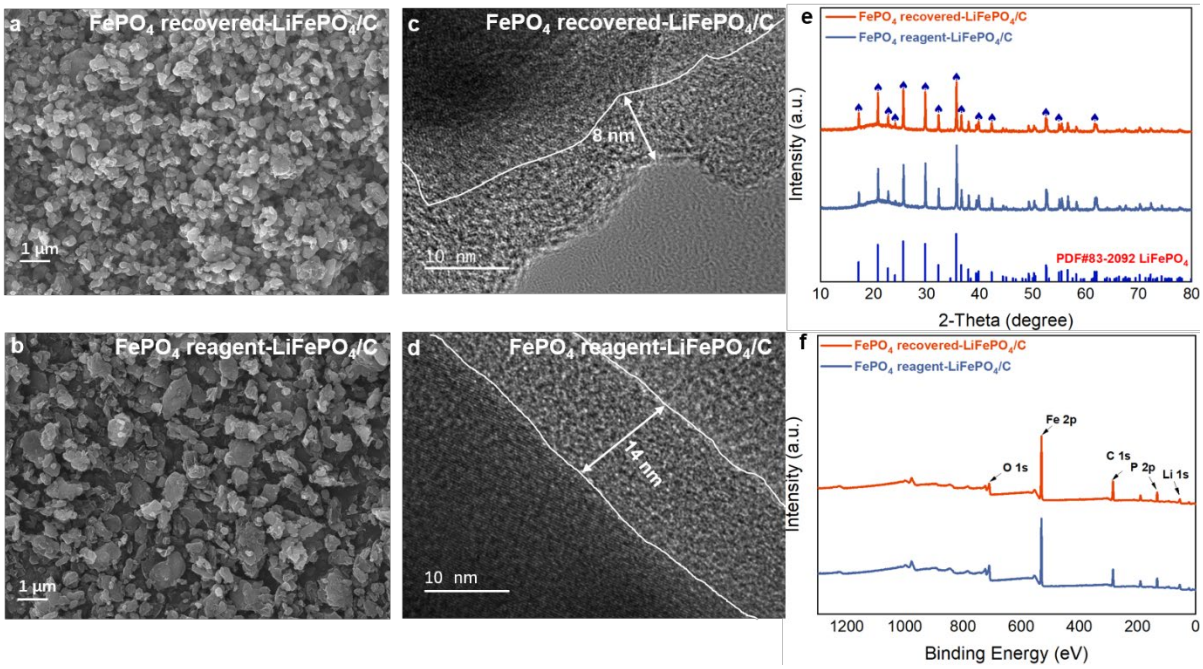


Fig. 4. Characterization of the $LiFePO_4$/C cathode materials for the comparison between (a, c) the recovered $FePO_4$ and (b, d) reagent $FePO_4$ using SEM (a, b) and TEM (c, d), and (e) XRD, and (f) wide-scan XPS.

3.3.2 Electrochemical performance of the $LiFePO_4$/C cathode

The electrochemical properties of the $LiFePO_4$/C cathodes using the recovered $FePO_4$ were compared to those using a commercial $FePO_4$ reagent. The initial specific discharge capacity of the synthesized $LiFePO_4$/C cathode at a C-rate of 0.1C reached 151 ± 2 mAh/g, which was not significantly different from the 148 ± 2 mAh/g observed for the reagent-based $LiFePO_4$/C cathode ($p = 0.14$) (Fig. 5a). The cathodes prepared using the recovered $FePO_4$ had better performance than those previously reported by Chen et al. (2022) of 136 mAh/g from spent LFP batteries and 37.3-107 mAh/g from wastewater sludge (Table 1). Charge–discharge curves of both cathode samples showed

a typical voltage plateau at ~3.4 V, corresponding to the characteristics of Li^+ intercalation/deintercalation between the $LiFePO_4$ and $FePO_4$ phases (Zhou et al., 2017).

The cathodes with the recovered $FePO_4$ also exhibited good long-term cyclic performance at 0.1C based on testing over 50 cycles (Fig. 5b), with slightly higher capacity retention efficiency of 96.7% compared to 92.6% for the commercial material. The $LiFePO_4$/C cathodes prepared from the recovered $FePO_4$ retained a higher discharge capacity of 143±1 mAh/g than the reagent-based cathode (140±2 mAh/g) after 50 cycles. The higher purity and the more uniform and smaller particle size of the $FePO_4$ precursors were likely responsible for the more stable electrochemical performance (Wang et al., 2019; Akhmetova et al., 2024). Cathodes using the Fe-P precipitate without sintering for purification had much poorer performance with an initial specific discharge capacity of only 125±2 mAh/g (Fig. 5).

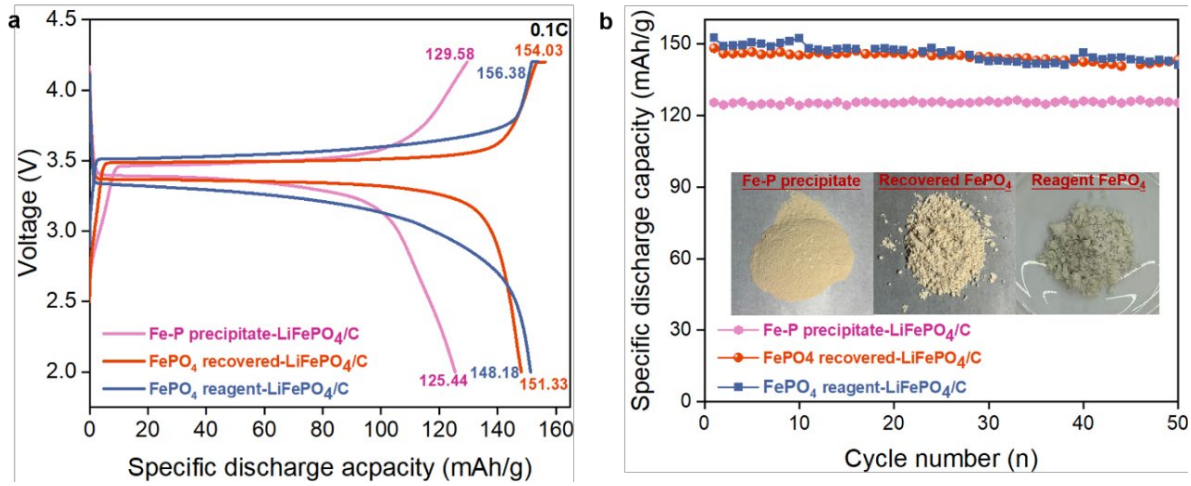


Fig. 5. Battery performance of the $LiFePO_4$/C cathodes synthesized using the different Fe-P precursors, including the recovered Fe-P precipitate, sintered $FePO_4$ product, and chemical reagent $FePO_4$: (a) initial charge/discharge curves under 2.0–4.2 V at 0.1C, (b) cyclic performance at 0.1C (inset: apparent morphology of the different Fe-P precursors).

Table 1. $FePO_4$ recovery and its corresponding $LiFePO_4$/C electrochemical performance.

P source	Fe source	Leaching reagents	P recovery efficiency (%)	Purity of $FePO_4$ (%)	LFP/C cathode (mAh/g)	Reference
Incinerated sludge ash	$FeCl_3$	H_2SO_4	99.6%	92.9%	–	Hu et al., 2023
Municipal wastewater (0.2 mg-P/L)	$FeCl_3$	Fe-NH_2-polyacrylonitrile (PAN) adsorbent +H_2SO_4	88.5%	91.4%-96.3%	37.3-55.8	Zheng et al., 2023
Slaughterhouse wastewater (48.9 mg-P/L)			91.3%	82.7%		
Slurry from sludge			75%	97.2-98.1%	100.4-106.7	Zou et al., 2024

anaerobic digestion						
Slurry from sludge anaerobic digestion	Polymerized ferrous sulfate (PFS) (Fe ⩾ 21%)	H_2SO_4	94.8%	93.5 %	82.5-100.4	Wang et al., 2024
Fe-enhanced primary sedimentation sludge	No chemicals	Food waste (No chemicals)	81% P	99.3%	151.3	This study

3.4 Significance for clean energy and environmental sustainability

There are several economic incentives for using the recovered $FePO_4$ to produce $LiFePO_4$ electrodes that include its high value relative to other products, and decreased overall carbon emissions. The $FePO_4$ material produced is equal to, or of a higher quality, than the commercial material tested here. The recovered $FePO_4$ is greater value as a source for electrode materials ($3,200/t) compared to recovery of P for use in fertilizers ($300/t). Mg addition is also typically required to make struvite-type fertilizers, which is an additional cost not required for producing $FePO_4$.

Possible additional economic benefits based of the $FePO_4$ were investigated using the EverBatt model developed by Argonne National Laboratory (Dai et al., 2019). For the production of $LiFePO_4$ cathodes, using $FePO_4$ recovered from the P-rich primary sludge reduced the costs by $3,470/t–$4,164/t compared to using mined P and Fe when considering costs due to P mining and its transportation, and it decreased the carbon emission by 0.4–0.5 ton CO_2/t with an energy saving of 30,560 MJ/t–36,672 MJ/t (Table 2). By using Fe-facilitated primary sedimentaion for organic and P removal, up to 95% of P in raw wastewater can be captured into FEPS (Lin et al., 2017b). Taking into account the release of P during sludge fermentation (82%) and the subsequent Fe-P precipitation efficiency (79% Fe and 81% P) obtained in this study, the overall efficiency of P recovery from municipal wastewater would be as high as 63% to produce high-quality $FePO_4$ for the $LiFePO_4$ cathodes. In 2021, the total amount of urban wastewater discharge in China was 62,507 million m^3, containing approximately 250,030 tons of P (MOHURD, 2022). With the 66% recovery ratio of P from wastewater established in this study, approximately 790,700 tons of $FePO_4$ would be produced, which would potentially supply 106% of $FePO_4$ for the LFP battery industry in China. As a result, 1.9 million tons (at 20 wt% P_2O_5) of natural P ore could be saved, approximately 38% of China's annual phosphorus consumption for fertilizers (5.0 Mt in 2017) (Gong et al., 2025). The analysis highlights the economic viability, as well as the environmental sustainability, of P recovery from wastewater sludge. The $LiFePO_4$/C cathodes synthesized from the recovered $FePO_4$ could be used for LFP batteries in large-scale energy storage systems, where decommissioned power batteries are commonly used (45–120 mAh/g) (Martinez-Laserna et al., 2018). This amount of $FePO_4$ if recovered from wastewater treatment plants in China would be sufficient to meet its current domestic LFP battery production (Fig. 6). By using this recovered $FePO_4$, natural phosphate resources could be conserved, thus providing benefits of both avoiding P extraction and

providing a recycled and clean-energy supply for the ever-growing energy storage industry.

Table 2. Cost-benefit analysis performed with the EverBatt model (Lou et al., 2021): comparison of (i) the proposed P recovery from FEPS with (ii) virgin P manufacturing for LFP production and (iii) P recovery from WBS for P-fertilizers (Desmidt et al., 2015; Egle et al., 2016; Pradel et al., 2019).

Method	Energy consumption (MJ/t)	CO_2 emission (kg CO_2-eq/t)	Cost ($/t)	Revenue ($/t)
(i) P recovery from FEPS for LFP cathodes	91,980 - 110,376	7,538 - 9,046	20,000 - 24,000	8,100 - 9,720
(ii) Virgin P manufacturing for LFP cathodes	122,540 - 147,048	7,951 - 9,541	23,470 - 28,164	5,500 - 6,600
(iii) P recovery from WBS for P-fertilizers	80,417 - 108,024	16,000 - 17,778	6,420 - 10,700	-745 - -1,100

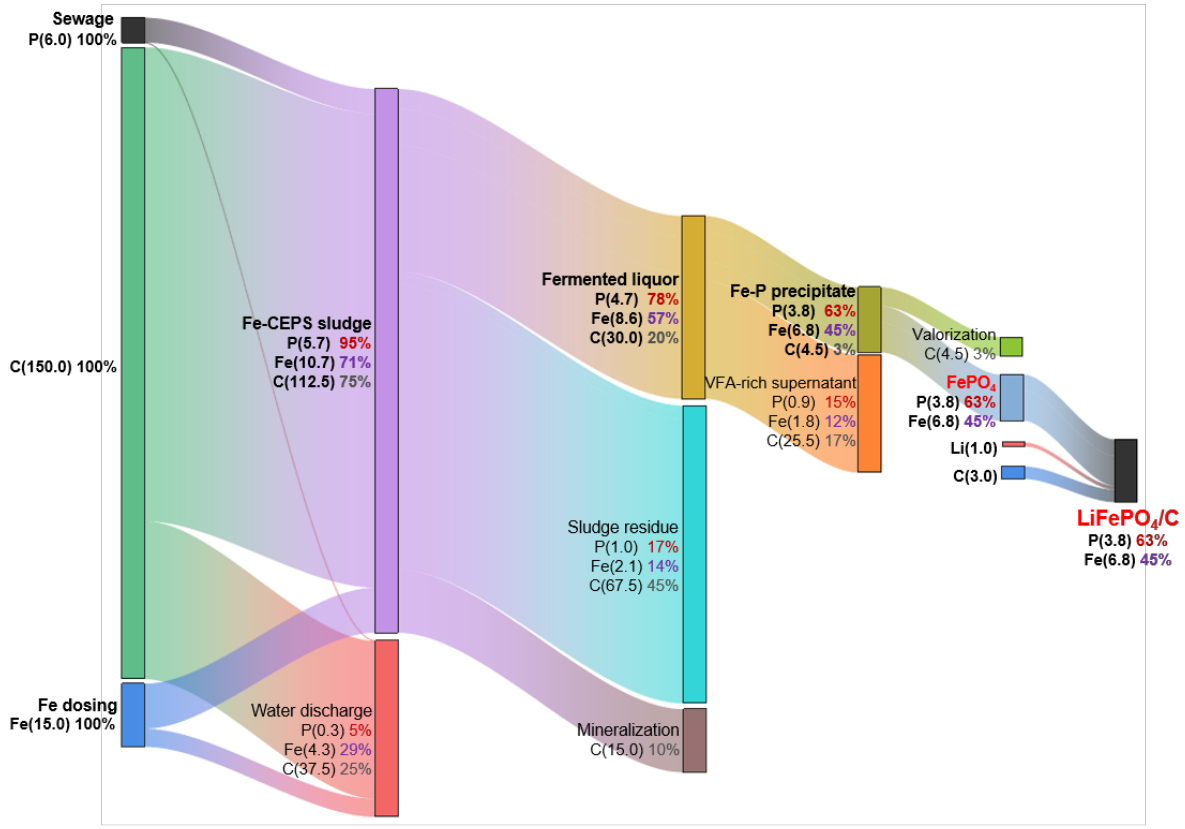


Fig. 6. Material flow analyses for P and C from wastewater and Fe throughout the proposed treatment system, with the amounts and percentages of the materials and products indicated (values in brackets are the amounts of materials in tons for 1 million m^3 of wastewater).

4. Conclusions

A new and sustainable method was shown to be effective for recovering P and Fe from wastewater sludge to produce $FePO_4$ for LFP batteries. Up to 82% of P was dissolved via acidogenic fermentation from the P-capturing primary sludge into the

supernatant to reach a high concentration of 149±2 mg-P/L. Precise regulation of the solution pH at 2.0 and a strong oxidative condition with H_2O_2 in the fermented supernatant resulted in re-precipitation of P with Fe, achieving a P recovery efficiency of 81% with little metal impurities. Through sintering of the Fe-P precipitate for product refining, the precipitate was transformed into crystalline $FePO_4$ with a high purity of 99.3%. The $LiFePO_4$/C cathode prepared from the recovered $FePO_4$ exhibited an excellent specific discharge capacity of 148 ± 3 mAh/g after 50 cycles at 0.1C, comparable to the performance of chemical reagent-based cathodes. The battery-grade $FePO_4$ is a more value-added P recovery product than P-fertilizers. Overall, the research findings provide a viable and sustainable method for P recovery with considerable economic gains from P-rich sludge and similar wastes for LFP batteries, benefiting resource conservation, environmental protection, and clean and renewable energy applications.

CRediT authorship contribution statement

Xuan Wang: Conceptualization, Formal analysis, Investigation, Data curation, Visualization, Writing - original draft, Writing - review & editing. **Yijiao Chang:** Methodology, Investigation. **Zhu Liang:** Methodology, Investigation, Data curation. **Anjie Li:** Validation, Supervision. **Yiru Wu:** Investigation, Validation. **Bohua Wen:** Formal analysis, Visualization. **Bing Li:** Resources, Supervision. **Feiyun Sun:** Visualization. **Xiao-yan Li:** Conceptualization, Writing - review & editing, Funding acquisition. **Bruce E. Logan:** Conceptualization, Formal analysis, Writing - review & editing. **Lin Lin:** Conceptualization, Supervision, Writing - original draft, Writing - review & editing, Project administration.

Declaration of competing interest

Authors declare no conflict of interest.

Data availability

Data will be made available on request.

Acknowledgments

This research was financially supported by the National Key Research and Development Program of China (Grant 2024YFC3906700), the National Natural Science Foundation of China (Grants 52270128 and 52261135627), the Basic and Applied Basic Research Foundation of Guangdong Province (Grant 2023A1515011734), and the Municipal Science and Technology Innovation Commission of the Shenzhen Government (Grants KCXFZ20211020163556020, SGDX20230116092359002, JCYJ20220818101006013).

Supplementary materials

Supplementary material associated with this article can be found in the online version.

References

Akhmetova, K., Sultanov, F., Mentbayeva, A., Umirov, N., Bakenov, Z. and Tatykayev, B. 2024. Advances in multi-element doping of $LiFePO_4$ cathode material for capacity enhancement in Li-ion batteries. J. Power Sources. 624, 235531. https://doi.org/10.1016/j.jpowsour.2024.235531

APHA 2005. Standard methods for the examination of water and wastewater, 21st Ed. American Public Health Association, Washington, DC, USA.

Bahgat, N.T., Siddiqui, A., Wilfert P., Korving, L. and Loosdrecht, V.M. 2024. $FePO_4{\cdot}2H_2O$ recovery from acidic phosphate-rich waste streams. Water Res. 260: 121905. https://doi.org/10.1016/j.watres.2024.121905

Boonchom, B. and Puttawong, S. 2010. Thermodynamics and kinetics of the dehydration reaction of $FePO_4{\cdot}2H_2O$. Physica B. 405(9), 2350-2355. http://doi.org/10.1016/j.physb.2010.02.046

Chang, Y., Wang, X., Zhao, B., Li, A., Wu, Y., Wen, B., Li, B., Li, X.Y. and Lin, L. 2024. Green and high-yield recovery of phosphorus from municipal wastewater for $LiFePO_4$ batteries. Engineering. 45: 234-242. https://doi.org/10.1016/j.eng.2024.05.018

Chen, B., Liu, M., Cao, S., Chen, G., Guo, X. and Wang, X. 2022. Regeneration and performance of $LiFePO_4$ with Li_2CO_3 and $FePO_4$ as raw materials recovered from spent $LiFePO_4$ batteries. Mater. Chem. Phys. 279, 125750. http://doi.org/10.1016/j.matchemphys.2022.125750

Chowdhury, R.B., Moore, G.A., Weatherley, A.J. and Arora, M. 2017. Key sustainability challenges for the global phosphorus resource, their implications for global food security, and options for mitigation. J. Clean Prod. 140, 945-963. https://doi.org/10.1016/j.jclepro.2016.07.012

CNMIA. 2024. China Nonferrous Metals Industry Association. https://www.chinania.org.cn/html/zhongguoyousejinshugongyexiehu/fenzhijigou/2022/1206/102.html

Dai, Q., Spangenberger, J., Ahmed, S., Gaines, L., Kelly, J.C. and Wang, M. 2019. EverBatt: A closed-loop battery recycling cost and environmental impacts model, Argonne National Laboratory (ANL), Argonne, IL (United States). https://doi.org/10.2172/1530874

Desmidt, E., Ghyselbrecht, K., Zhang, Y., Pinoy, L., Van der Bruggen, B., Verstraete, W., Rabaey, K. and Meesschaert, B. 2015. Global phosphorus scarcity and full-scale P-recovery techniques: a review. Crit Rev Env Sci Tec, 45(4), 336-384. https://doi.org/10.1080/10643389.2013.866531

Dunn, J.B. 2024. The balancing act of turning wastes into feedstocks. Nat. Synth. 3(7), 790-791. https://doi.org/10.1038/s44160-024-00579-5

Egle, L., Rechberger, H., Krampe, J. and Zessner, M. 2016. Phosphorus recovery from municipal wastewater: An integrated comparative technological, environmental and economic assessment of P recovery technologies. Sci. Total Environ, 571, 522-542.

https://doi.org/10.1016/j.scitotenv.2016.07.019

Fan, E., Li, L., Wang, Z., Lin, J., Huang, Y., Yao, Y., Chen, R. and Wu, F. 2020. Sustainable recycling technology for Li-ion batteries and beyond: challenges and future prospects. Chem. Rev. 120(14), 7020-7063. http://doi.org/10.1021/acs.chemrev.9b00535

Gong, H., Yin, Y., Chen, Z., Zhang, Q.S., Tian, X.S., Wang, Z.H., Wang Y.C. and Cui, Z.L. 2025. A dynamic optimization of soil phosphorus status approach could reduce phosphorus fertilizer use by half in China. Nat Commun. 16(1): 976. https://doi.org/10.1038/s41467-025-56178-1

Hu, S., Yi, K., Li, C., Ma, S., Liu, J. and Yang, W. 2023. Efficient and selective recovery of iron phosphate from the leachate of incinerated sewage sludge ash by thermally induced precipitation. Water Res. 238, 120024. http://doi.org/10.1016/j.watres.2023.120024

Laouini, E., Moukhliss, Y., Oukhrib, R., Kachbou, Y., Albrimi, Y.A., Alahiane, M., Akbour, R.A., Marbrouk, A., Bachar, A., Assabbane, A., Nahle, A., Hammouti, B. and Hamdani, M. 2025. Synthesis, characterization, and electrochemical performance of amorphous and crystalline $FePO_4$ used as cathode materials in aqueous lithium-ion electrolyte. Moroc. J. Chem. 13(1), 205-229. https://doi.org/10.48317/IMIST.PRSM/morjchem-v13i1.52947

Lee, C., Truong, H., Ngo, K.N., AlSayed, A., Kin, E.K., Fuentes, S., Chen, X.J., Clippeleir, H. D. and Wells, G. 2025. Integrating biological phosphorus removal with high-rate activated sludge for enhanced settleability and nutrient management at short solids retention times. ACS. EST. Engg. https://doi.org/10.1021/acsestengg.4c00524

Li, C., Sheng, Y. and Xu, H. 2021. Phosphorus recovery from sludge by pH enhanced anaerobic fermentation and vivianite crystallization. J. Environ. Chem. Eng. 9(1), 1. http://doi.org/10.1016/j.jece.2020.104663

Li, M., Lu, J., Chen, Z. and Amine, K. 2018. 30 years of lithium-ion batteries. Adv. Mater. 30, e1800561. http://doi.org/10.1002/adma.201800561

Li, R.H., Cui, J.L., Hu, J.H., Wang, W.J., Li, B., Li, X.D. and Li, X.Y. 2020. Transformation of Fe-P complexes in bioreactors and P recovery from sludge: investigation by XANES spectroscopy. Environ. Sci. Technol. 54(7), 4641-4650. http://doi.org/10.1021/acs.est.9b07138

Li, R.H., Cui, J.L., Li, X.D. and Li, X.Y. 2018a. Phosphorus removal and recovery from wastewater using Fe-dosing bioreactor and co-fermentation: investigation by X-ray absorption near-edge structure spectroscopy. Environ. Sci. Technol. 52(24), 14119-14128. http://doi.org/10.1021/acs.est.8b03355

Li, R.H., Wang, W.J., Li, B., Zhang, J.Y., Liu, J., Zhang, G.J., Guo, X.C., Zhang, X.H. and Li, X.Y. 2019. Acidogenic phosphorus recovery from the wastewater sludge of the membrane bioreactor systems with different iron-dosing modes. Bioresour. Technol. 280, 360-370. http://doi.org/10.1016/j.biortech.2019.02.060

Li, R.H., Wang, X.M. and Li, X.Y. 2018b. A membrane bioreactor with iron dosing and acidogenic co-fermentation for enhanced phosphorus removal and recovery in wastewater treatment. Water Res. 129, 402-412. http://doi.org/10.1016/j.watres.2017.11.035

Liao, Q., Sun, L., Lu, H., Qin, X., Liu, J., Zhu, X., Li, X.Y., Lin, L. and Li, R.H. 2024. Iron driven organic carbon capture, pretreatment, recovery and upgrade in wastewater:

Process technologies, mechanisms, and implications. Water Res. 122173. https://doi.org/10.1016/j.watres.2024.122173

Lin, L., Li, R.H., Li, Y., Xu, J. and Li, X.Y. 2017a. Recovery of organic carbon and phosphorus from wastewater by Fe-enhanced primary sedimentation and sludge fermentation. Process Biochem. 54, 135-139. http://doi.org/10.1016/j.procbio.2016.12.016

Lin, L., Li, R.H., Yang, Z.Y. and Li, X.Y. 2017b. Effect of coagulant on acidogenic fermentation of sludge from enhanced primary sedimentation for resource recovery: Comparison between $FeCl_3$ and PACl. Chem. Eng. J. 325, 681-689. http://doi.org/10.1016/j.cej.2017.05.130

Lou, W.B., Zhang, Y., Zhang, Y., Zheng, S.L., Sun, P., Wang, X.J., Qiao, S., Li, J.Z., Zhang, Y., Liu, D.Y., Wenzel, M. and Weigand, J.J. 2021. A facile way to regenerate $FePO_4{\cdot}2H_2O$ precursor from spent lithium iron phosphate cathode powder: spontaneous precipitation and phase transformation in an acidic medium. J. Alloys Compd. 856, 158148. http://doi.org/10.1016/j.jallcom.2020.158148

Lovley, D.R. and Phillips, E.J. 1988. Novel mode of microbial energy metabolism: organic carbon oxidation coupled to dissimilatory reduction of iron or manganese. Appl. Environ. Microbiol. 54(6), 1472-1480. https://doi.org/10.1128/aem.54.6.1472-1480.1988

Mao, C., Feng, Y., Wang, X. and Ren, G. 2015. Review on research achievements of biogas from anaerobic digestion. Renew. Sust. Energ. Rev. 45, 540-555. http://doi.org/10.1016/j.rser.2015.02.032

Martinez-Laserna, E., Gandiaga, I., Sarasketa-Zabala, E., Badeda, J., Stroe, D.-I., Swierczynski, M. and Goikoetxea, A. 2018. Battery second life: hype, hope or reality? A critical review of the state of the art. Renew. Sust. Energ. Rev. 93, 701-718. https://doi.org/10.1016/j.rser.2018.04.035

Meng, X., Huang, Q., Gao, H., Tay, K. and Yan, J. 2018. Improved utilization of phosphorous from sewage sludge (as Fertilizer) after treatment by low-temperature combustion. Waste Manage. 80, 349-358. https://doi.org/10.1016/j.wasman.2018.09.034

MOHURD. 2022. Ministry of Housing and Urban-Rural Development of the People's Republic of China. China Urban Construction Statistical Yearbook. Beijing: China Statistics Press. https://www.mohurd.gov.cn/gongkai/fdzdgknr/sjfb/tjxx/index.html

Ouikhalfan, M., Lakbita, O., Delhali, A., Assen, A.H. and Belmabkhout, Y. 2022. Toward net-zero emission fertilizers industry: greenhouse gas emission analyses and decarbonization solutions. Energy Fuels. 36(8), 4198-4223. http://doi.org/10.1021/acs.energyfuels.2c00238

Phan, A.T., Gheribi, A.E. and Chartrand, P. 2019. Modeling of coherent phase transformation and particle size effect in $LiFePO_4$ cathode material and application to the charging/discharging process. Electrochim. Acta. 295, 632-644. https://doi.org/10.1016/j.electacta.2018.10.185

Pokhrel, S., Milke, M., Bello-Mendoza, R., Buitrón, G. and Thiele, J.J.W.M. 2018. Use of solid phosphorus fractionation data to evaluate phosphorus release from waste activated sludge. Waste Manage. 76, 90-97. https://doi.org/10.1016/j.wasman.2018.03.008

Pradel, M., Aissani, L. 2019. Environmental impacts of phosphorus recovery from a “product” life cycle assessment perspective: allocating burdens of wastewater treatment in the

production of sludge-based phosphate fertilizers. Sci Total Environ, 656, 55-69. https://doi.org/10.1016/j.scitotenv.2018.11.356

Song, Y., Chen, Q., Zhang, H., Zhang, S., Zhang, K., Hu, J., Li, Y. and Yao, Y. 2025a. Adenosine triphosphate in solvothermal method for preparing high-rate $LiFePO_4$ cathode material. Mater Today Chem. 45: 102659. https://doi.org/10.1016/j.mtchem.2025.102659

Song, Y., Zhang, W., Li, Y., Yao, Y., Dong, Z. and Yuan, L. 2025b. Resource utilization of iron ore concentrate leachate: Constructing polyacrylonitrile-coated Fe_2O_3 core-shell structures for optimized lithium storage performance. J. Energy Storage. 136: 118462. https://doi.org/10.1016/j.est.2025.118462

Taboada-Santos, A., Rivadulla, E., Paredes, L., Carballa, M., Romalde, J. and Lema, J.M. 2020. Comprehensive comparison of chemically enhanced primary treatment and high-rate activated sludge in novel wastewater treatment plant configurations. Water Res. 169, 115258. https://doi.org/10.1016/j.watres.2019.115258

Taddeo, R., Honkanen, M., Kolppo, K. and Lepisto, R. 2018. Nutrient management via struvite precipitation and recovery from various agroindustrial wastewaters: process feasibility and struvite quality. J. Environ. Manage. 212, 433-439. http://doi.org/10.1016/j.jenvman.2018.02.027

Tu, J., Chen, L., Li, Y., Wang, X. and Zhang, B. 2025. Effect of carbon sources on the microstructure and performance of $LiFePO_4$ microspheres from hydrous $FePO_4$. J. Alloys Compd. 179168. https://doi.org/10.1016/j.jallcom.2025.179168

Uysal, A., Yilmazel, Y.D. and Demirer, G.N. 2010. The determination of fertilizer quality of the formed struvite from effluent of a sewage sludge anaerobic digester. J. Hazard. Mater. 181(1-3), 248-254. http://doi.org/10.1016/j.jhazmat.2010.05.004

Van Loosdrecht, M.C. and Brdjanovic, D. 2014. Anticipating the next century of wastewater treatment. Science 344(6191), 1452-1453. 10.1126/science.1255183

Veeken, A. and Hamelers, H. 1999. Removal of heavy metals from sewage sludge by extraction with organic acids. Water Sci. Technol. 40(1), 129-136. https://doi.org/10.1016/S0273-1223(99)00373-X

Wang, J.J. and Sun, X.L. 2012. Understanding and recent development of carbon coating on $LiFePO_4$ cathode materials for lithium-ion batteries. Energy Environ. Sci. 5(1), 5163-5185. http://doi.org/10.1039/c1ee01263k

Wang, Q., Kim, T.H., Reitzel, K., Almind-Jørgensen, N. and Nielsen, U. G. 2021. Quantitative determination of vivianite in sewage sludge by a phosphate extraction protocol validated by PXRD, SEM-EDS, and ^{31}P NMR spectroscopy towards efficient vivianite recovery. Water Res. 202, 117411. https://doi.org/10.1016/j.watres.2021.117411

Wang, X., McCarty, P.L., Liu, J., Ren, N.Q., Lee, D.J., Yu, H.Q., Qian, Y. and Qu, J. 2015. Probabilistic evaluation of integrating resource recovery into wastewater treatment to improve environmental sustainability. Proc. Natl. Acad. Sci. 112(5), 1630-1635. https://doi.org/10.1073/pnas.1410715112

Wang, Y., Fei, R.X., Yuan, Z.H., Li, Y.J., Zhang, H.C. and Li, J. 2024. Low-carbon emitting Fe-cycle recovery of battery-grade $FePO_4$ from biogas slurry for Li-battery application. Chem Eng J. 496: 154131. https://doi.org/10.1016/j.cej.2024.154131

Wang, Z. and Lu, Y. 2019. Facile construction of high-performance amorphous $FePO_4$/carbon

nanomaterials as cathodes of lithium-ion batteries. ACS Appl. Mater. Interfaces. 11(14), 13225-13233. https://doi.org/10.1021/acsami.8b22720

Wu, Y., Luo, J., Zhang, Q., Aleem, M., Fang, F., Xue, Z. and Cao, J. 2019. Potentials and challenges of phosphorus recovery as vivianite from wastewater: a review. Chemosphere. 226, 246-258. https://doi.org/10.1016/j.chemosphere.2019.03.138

Xue, T.Z., Dong, B., Li, W.H., Yang, H.Y., Yang, X.L. 2025. Phosphorus recovery and microbial community analysis during anaerobic co-fermentation of excess sludge and food waste. J Envir Chem Eng. 117398. https://doi.org/10.1016/j.jece.2025.117398

Yin, Z., Liu, H., Fu, L., Jiang, F., Pei, J., Wang, S., Li, Z., Zhang, G. and Zhang, L. 2025. Constructing advanced oxidation field by ultrasound towards separation of lithium from spent lithium iron phosphate. Chem Eng J. 167076. https://doi.org/10.1016/j.cej.2025.167076

Yuan, Y., Hu, J., Wang, L., Li, Y. and Yao, Y. 2024. Structural properties and electrochemical performance of different polymorphs of $FePO_4$ as raw materials for lithium ion electrodes. J. Mater. Chem. C. 12(18), 6511-6518. 10.1039/D4TC00957F

Zeng, L., Li, X., Shi, Y., Qi, Y., Huang, D., Tade, M., Wang, S. and Liu, S. 2017. $FePO_4$ based single chamber air-cathode microbial fuel cell for online monitoring levofloxacin. Biosens Bioelectron. 91, 367-373. http://doi.org/10.1016/j.bios.2016.12.021

Zhang, B., Wang, L. and Li, Y. 2019. Fractionation and identification of iron-phosphorus compounds in sewage sludge. Chemosphere. 223, 250-256. http://doi.org/10.1016/j.chemosphere.2019.02.052

Zhang, Q., Li, X., Wang, Q. and Wang, S. 2022. Low-temperature solid-state synthesis of $FePO_4$ as a heterogeneous fenton-like catalyst for the degradation of methyl blue. J. Appl. Spectrosc. 89, 170–176. https://doi.org/10.1007/s10812-022-01340-6

Zheng, K., Wang, Y., Xiang, L., Huang, C., Zhang, H. and Li, J. 2023. A dual-cycle regeneration to recover high-value and high-purity $FePO_4$ from real wastewater for Li-battery application. Water Res. 242, 120300. http://doi.org/10.1016/j.watres.2023.120300

Zheng, M., Hu, Z., Liu, T., Sperandio, M., Volcke, E.I., Wang, Z., Hao, X., Duan, H., Vlaeminck, S.E. and Xu, K. 2024. Pathways to advanced resource recovery from sewage. Nat. Sustain. 7(11), 1395-1404. https://doi.org/10.1038/s41893-024-01423-6

Zhou, D., Qiu, X., Liang, F., Cao, S., Yao, Y., Huang, X., Ma, W., Yang, B. and Dai, Y. 2017. Comparison of the effects of $FePO_4$ and $FePO_4{\cdot}2H_2O$ as precursors on the electrochemical performances of $LiFePO_4$/C. Ceram. Int. 43(16), 13254-13263. http://doi.org/10.1016/j.ceramint.2017.07.023

Zhou, L., Chen, J., Qian, Y., Zhang, Y., Batjargal, E., Tuulaikhuu, B. A. and Zhou, X. 2025. Unlocking phosphorus recovery from microalgae biomass: the enhanced transformation and release of phosphorus species. Water Res. 123196. https://doi.org/10.1016/j.watres.2025.123196

Zhu, Y.M., Ruan, Z.W., Tang, S.Z. and Thangadurai V. 2014. Research status in preparation of $FePO_4$: a review. Ionics. 20(11), 1501-1510. http://doi.org/10.1007/s11581-014-1241-x

Zou, J., Zhang, H., Zheng, K. and Li, J. 2024. Pilot-scale phosphorus recovery from biogas slurry to produce battery-grade $FePO_4$: Chemical enhanced primary treatment coupled adsorption process. Sep. Purif. Technol. 348. http://doi.org/10.1016/j.seppur.2024.127677